

Analysis of GaN based high-power diode lasers after singular degradation events

Giovanna Mura,¹⁾ Massimo Vanzi,¹⁾ Martin Hempel,^{2,3)} Jens W. Tomm^{2,a)}

¹⁾ *Department of Electrical and Electronic Engineering, University of Cagliari, 09124 Cagliari, Italy*

²⁾ *Max-Born-Institut für Nichtlineare Optik und Kurzzeitspektroskopie, Max Born Str. 2A, Berlin D-12489, Germany*

³⁾ *Currently with the Paul Drude Institut, Hausvogteiplatz 5-7, 10117 Berlin, Germany*

Abstract

Damage pattern caused by the Catastrophic Optical Damage (COD) in GaN-based high-power diode lasers are analyzed. In contrast to standard failure analysis, the devices have been intentionally degraded under well-defined conditions. We find that defect growth during COD is feed by the optical mode; i.e. laser energy. It is a process that involves melting and even vaporization of MQW and waveguide materials. This indicates the presence of temperatures on the order of 2500-3000°C. Defect propagation velocities along the laser axis of 110 m/s are observed. COD results in material loss including the formation of an empty channel, which is well consistent with material loss due to ejections of hot material out of the front facet of the device. The laser structure in the immediate vicinity of the empty channel seems to be absolutely undisturbed and no transition regions or remaining material are observed. These facts are compared with earlier findings from comparable experiments with GaAs-based devices.

"This is the pre-peer reviewed version of the following article:

Mura, G., Vanzi, M., Hempel, M. and Tomm, J.W. (2017), Analysis of GaN based high-power diode lasers after singular degradation events, which has been published in final form at Phys. Status Solidi RRL, 11: 1700132. <https://doi.org/10.1002/pssr.201700132>.

This article may be used for non-commercial purposes in accordance with Wiley Terms and Conditions for Use of Self-Archived Versions."

a) Corresponding author tomm@mbi-berlin.de, <http://www.mbi-berlin.de/de/research>

1. Introduction

GaN-based light emitting diodes and diode lasers are the main optoelectronic light sources for the visible and ultraviolet spectral regions. In recent years, their performance underwent tremendous improvements. For a number of reasons, however, the power (density) levels achieved by GaN-based diode lasers are still lower than those reached by their GaAs-based relatives. A discussion of these reasons is beyond the scope of this report. The mere fact, however, explains why many *effects typical for high-power operation* of diode lasers have not found a lot of attention in the literature on GaN-based diode lasers, up to now.

The *catastrophic optical damage* (COD) effect is a generic degradation effect related to high power densities.¹ It is well studied for GaAs-based diode lasers,¹⁻³ and at least observed for GaN-based devices, as well.⁴⁻⁸ Therefore it is relevant, and its relevance will increase when the power levels will further advance. COD takes place in all materials through which high photon fluxes are transmitted,³ e.g. waveguides. If there is any absorbing site within the material, a defect or a tiny structural inhomogeneity, this might lead to an increased local temperature, which can boost the local absorption at this particular site. Local absorption of light leads to local warming. This describes a feedback loop,¹ which can eventually create localized microscopic degradation seeds consisting of, e.g., *accumulations of point defects*, which represent potential starting points of COD. In GaAs-based devices, COD has been originally observed at front facets of edge-emitting devices.⁹ With the advent of advanced facet passivation and coating technologies,² this bottleneck was eliminated and imperfection *within the waveguides* became primary starting points for COD.^{10, 11} Independent on the starting point, surfaces or bulk, the COD scenario, a positive feedback loop, remains always the same. Moreover, COD is an effect that cannot be eliminated, but only *delayed towards higher photon densities*. Therefore, the understanding of this effect is of fundamental interest, far beyond the analysis of degradation effects, which might be relevant, for a specific device design or specific operation conditions, only.

In this Letter, we provide a quantitative study of the COD effect in GaN-based high-power diode lasers with the main focus to the analysis of the damage pattern. In contrast to standard *failure analysis*, this device has been intentionally degraded in a way that the amount of energy introduced into the damage site is known. Both operation time and the duration of the degradation event are known, as well. This allows, e.g., estimates about temperature during failure and the corresponding sequences of events. Moreover, the actual data allow a comparison between COD in GaAs- and GaN-based devices, which completes our report.

2. Experimental

The experimental setup used for the tests has been introduced in Ref.⁴ We apply a *single-pulse step test* scheme with a fixed operation current pulse length of 800 ns. Starting with a current of 0.2 A, i.e., significantly below the COD threshold for this device and pulse length, we apply a single current pulse to the device. During this pulse, the transient behaviors of emission power, current, and voltage are monitored and stored at an oscilloscope. Then the current amplitude is increased by 0.4 A. This procedure is repeated as long as the device suddenly fails. In order to clearly identify all changes, each single pulse of increasing amplitude is followed by a standard 0.2-A *test pulse*. The evolution of the parameters taken during these test pulses clearly pinpoint, if present, the emergence of gradual degradation *en route* to the sudden event.

We investigated 450-nm-emitting PL TB450B devices in TO56 package, which are purchased from a commercial website.¹² These devices are based on an asymmetric multiple quantum-well (MQW) structure and feature a 15- μm wide emitter stripe on top of the p-side up packaged chips. The cavity length is 1.2 mm. A batch of 8 devices has been subjected to *single-pulse step tests* in a way similar to the one described in Ref.⁴ The particular device that is subject of the detailed analysis reported here has shown COD in the 13th pulse at ~ 5 A, and went before additionally through 12 single 0.2-A test pulses. When comparing the data from these test pulses, power-, current- and voltage-transients, we found no gradual changes *en route* to the sudden event. Thus, we conclude that all damage has been generated during the singular COD event in the 13th pulse that began 100 ns after the onset of the 800-ns pulse, as seen from the power transient. Comparing the shapes of such power transients, see Fig. 3 (c) in Ref.¹³, we estimate an energy of $W = (2 \pm 1) \mu\text{J}$, which was introduced into the COD-site within 700 ns. This number will be important in further considerations.

In an earlier report on sudden degradation of comparable GaN-based devices produced for research purposes,⁴ we performed a similar type of *COD preparation* and accompanied the process by additional analytical tools, in particular a thermo-camera, which took time-integrated snapshots during the single pulses. During the particular pulse, when the COD took place, an ejection of hot material out of the front facet has been clearly imaged by the thermo-camera. This observation was repeatedly made; with different pristine devices, of course. Therefore we assume that this is a typical behavior of this type of devices for the given operation conditions, not necessarily for long-term aging. Although we do not have unambiguous experimental evidence for material ejections for the present set of experiments, our earlier observations gives us reason to consider it extremely likely that the same type of degradation scenario took place here, as well. We will come back to this, when we discuss the details of the damage pattern.

The equipment for the Scanning Electron Microscopy (SEM) and Focused Ion Beam (FIB) observation and preparation has been a FEI Dual Beam Nova Nanolab 600. The instrument for TEM/STEM is a FEI Tecnai F20 ST, operated at 200 keV. For our investigations, we extracted 3 lamellas from the active region of the device. These lamellas represent x-z-planes as indicated by the red plane in the scheme in Fig. 1. Together, these three lamellas cover the entire x-z-cross section of the center of the active region from $z=0$ (front facet) to $z\sim 110\ \mu\text{m}$. This allows for a detailed inspection of the cross section of the macroscopic defect that has been caused by one singular COD event. The dimensions of the lamellas are about $40 \times 5 \times 1\ \mu\text{m}^3$. For the TEM investigations, the lamella thickness of about $1\ \mu\text{m}$ has been locally reduced down to $\sim 20\ \text{nm}$.

3. Results

Figure 1 (a) shows the outer appearance of the front facet of a diode laser after sudden degradation. It looks similar to what we⁴ and other authors^{6, 8} have published before. There are, however, two distinctions. First, Gallium droplets, which typically 'decorate' the surrounding of such pattern, are missing. We think that they got lost during the transfer between the labs. Second, there are cracks along the metallization of the emitter stripes; see red marks in Figure 1 (b). This particular type of cracking has not been observed for COD during long-term aging^{6, 8}. Therefore, we think, that the cracks along the metallization of the emitter stripe are result of the acceleration of the COD process by the single-pulse step test applied here. The ellipsoidal hole at the front, however, resembles exactly what is considered *typical COD pattern* of GaN-based devices, the topic of all our further considerations. It is a feature that has been investigated by the authors for devices made of the InP and GaAs material systems,¹⁴ and has been recalled in a recent paper on COD in InP-based emitters.¹⁵

Figure 2 (a) is an SEM image of the first lamella in the region of the front facet. The channel created by the COD-event in the optically active region is well visible. Figure 2 (b) shows the same region for a pristine reference device, which stems from the same lot as the degraded one shown in (a). In both subfigures, we marked the front facet by red lines. Figure 2 (c) shows a larger section of the first lamella. The first $\sim 5\ \mu\text{m}$ from the front facet along the z-axis of the channel are filled with material. The abundant presence of C and O instead of heavy Gallium or Indium here indicate, however, that this material is a subsequent contamination and not result of the COD process itself. This is supported by the dark contrast at the SEM picture of the facet; see Fig. 1 (a). If one compares all 3 subfigures, it becomes clear the deformation of the emitter stripe, i.e. the upwards-bend of the p-metallization and the cracks, which were already mentioned in the preceding section, is limited to the first $\sim 5\ \mu\text{m}$ along the z-axis. We think that this is the one and only peculiarity that has been caused by the

specific test methodology, while the remaining damage pattern represent the usual signature that accompanies COD in GaN-based devices.

Figure 3 (a) gives an overview image of the emitter stripe, where the second and third TEM lamellas have been extracted by FIB. The red arrow points to the end of the channel created by the COD-event. It is at $z \sim 80 \mu\text{m}$, i.e. in the third lamella. Figure 3 (b) shows this channel in more detail. If one compares its position along the x-axis (extension into p- and n-materials), as well as its thickness (total extension along x) with those in Figs. 2, one finds that the entire channel has an utmost high uniformity with regard to these two parameters along the entire z-axis from $z=0$ to $80 \mu\text{m}$. At this point we should mention that we checked this with lamella 2, as well. Lamella 2, however, is not further involved into the discussion, because it shows exclusively an extremely uniform and empty channel, comparable to what is visible in Fig. 3 (b) already.

Figures 4 show the details of the final section of this channel, taken by 200 keV STEM with highest resolution. These images clearly reveal the details of the epitaxial architecture as well as the respective position of the damage pattern. The MQWs are well resolved, see red arrow at the bright signature. The second red arrow at the darker signature above the MQW points to the electron blocking layer; compare this with Fig. 2 (c) in Friede et al.¹⁶ Obviously, the epitaxial architecture was designed in a way that the optical mode is predominantly guided in the less absorbing n-material instead of the p-side. Exactly this feature is well visible in the damage pattern shown in Fig. 4, where the QW acts as end point of the channel, see right red circle in Fig. 4 (b). Notice that the expansion of the channel towards p- and n-sides behaves like one by two. For obtaining Fig. 4 (b) by STEM, the sample was locally thinned down to about 20 nm. Nevertheless, the MQW is still clearly visible, even in the foreground of the damage channel, see left red circle in Fig. 4 (b). This is a location, where the total thickness of the sample in front of the channel is definitely substantially lower than 20 nm. This leads us to the statement that there is *almost no transition region* between the empty channel and the completely undisturbed epitaxial structure of the active region including the MQW. This is additionally supported by the continuation of the MQW into the undamaged material without any notable disruption; see right red circle in Fig. 4 (b).

Figures 1-4 provide, among others, detailed information about the geometry of the COD-induced channel. All in all, the dimensions of the damage site are $80 \mu\text{m}$ (length along z-axis), 400 nm (height) and $6.5 \mu\text{m}$ (width). While the first two numbers are taken directly from the SEM/TEM images, the latter is an estimate only, which has been obtained from the width of the ellipsoidal damage site (major axis) at the front facet; see Figs. 1. Thus, the volume of the empty channel amounts to $2.1 \times 10^{-10} \text{ cm}^3$. With an averaged density of 6.15 g/cm^3 , the mass of 'missing' material is $1.3 \times 10^{-9} \text{ g}$.

4. Discussion

We start with considering possible *scenarios* for the COD process on the base of the observed damage pattern. We assume that the process started at the front facet, i.e. at the interface between the semiconductor surface and the front facet passivation and coating layers. The arguments for this assumption are:

- The motion of hot spots starting at $z=0$ and moving along z has been directly verified for GaAs-based devices by *in situ* measurements.^{17, 18}
- In x -direction, the actually observed damage pattern resembles the extension of the optical mode. This points to the laser emission as driving force as well as supplier of energy for the damage extension; a situation similar again to the one in GaAs-based devices.¹ If this is right, any starting point at $0 < z < 800 \mu\text{m}$ would lead to a predominant motion of the defect rather towards larger z -values than to the front facet; see lines of arguments given in Ref. ¹⁹ Eventually, this should result in an undamaged region between $z=0$ and the assumed starting point at $z > 0$. Obviously, this is not observed here.

Another interesting issue is the *local temperature*, at which the fast kinetics of the COD process starts, i.e. where the *gradual aging turns into sudden degradation*, at least locally. From epitaxial growth (e.g. metal-organic chemical vapor deposition) it is known that at $\sim 1000^\circ\text{C}$ and ambient pressure, Gallium and Nitrogen atoms start leaving the GaN surface, eventually resulting in small Gallium droplets at the surface, while the Nitrogen vaporizes. A location at a surface altered in this way is expected to dramatically increase its local absorption and jumpstart the positive feedback loop described in section 1. Eventually this would lead to a temperature increase up to the melting point within $\sim 10 \text{ ns}$;^{20, 21} i.e. during ~ 500 roundtrips of the 450 nm laser light. An even higher local temperature for the jumpstart is unlikely, because at a local temperature of $\sim 1000^\circ\text{C}$ also the bandgap of GaN, representing a waveguide material, is lowered to an energy corresponding to the 450 nm emission wavelength.²² This would result in bulk-like interband absorption at the heated location and result again in melting on a ns-timescale in a way as described for early heterolasers.²¹ At the melting temperature of 2500°C ,²³ the stoichiometric GaN compound is expected to disassemble into liquid Gallium and gaseous Nitrogen. Taking into account the standard atomic weights of 14 and 70, and the density of gaseous Nitrogen of 1.251 g/l (ambient temperature), the bulk extension caused by the freed Nitrogen gas alone amounts to ~ 1200 generating a pressure that exceeds 1 kbar. Assuming the Nitrogen gas to be at $\sim 2500 \text{ K}$, the pressure rises by another order of magnitude. Obviously, this pressure is responsible for the observed

- cracks at the contact stripes, see Fig. 1 (a) and red marks in Fig. 1 (b), and
- material ejections,⁴ which most likely consist of liquid or even gaseous Gallium (boiling temperature $\sim 2700 \text{ K}$) and Nitrogen gas, which probably generates the pressure that could reach the 1-10 kbar-level.

Note that the actually small amounts of material 'missed' at the damage site, $\sim 0.2 \text{ ng}$ of Nitrogen and $\sim 1.1 \text{ ng}$ of Gallium, generate distinct thermo-camera signatures

~1 mm in length; see Ref.⁴ Although this alone is not sufficient to make temperature estimates, these numbers point to very high temperatures.

A more quantitative estimate of temperature is based on the energy that created the damage pattern, $W = (2 \pm 1) \mu\text{J}$. This energy was freed within ~700 ns. Assuming weak exchange with the surrounding, i.e. adiabatic boundary conditions, we presume that this amount of energy gets freed in the empty channel only. Taking into account the total mass of the 'missing' material of 1.3 ng and

$$W = m \times c \times \Delta T \quad (1)$$

As well as $c(\text{GaN}) = 0.49 \text{ J}/(\text{gK})$, we get $\Delta T = 3200 \text{ K}$ that indeed matches the order of the actual melting point of GaN of ~2500°C.²³ Thus we conclude that it is highly likely that the COD process in GaN-based devices involves material melting and even vaporization.

The extension of the damage pattern along the laser axis amounts to ~80 μm . Given that the COD has started at the front facet and lasted ~700 ns, we find an average propagation velocity along the laser axis of ~110 m/s. This value exceeds values of 30 m/s detected in accelerated step tests with 808 nm emitting GaAs-based devices under comparable conditions in terms of thermal load.¹³ For regular continuous wave operation 20 m/s have been detected for this material system.¹⁷ Whether the more than 3 times higher damage propagation velocity in the GaN-based device, compared to the GaAs-based one, is indeed a general feature or rather related to the particular device cannot be decided on the base of the currently available material.

All our data, including that presented in Figs. 1-4, shows no indication for the presence of any recrystallized material that could have been produced during the cool-down after damage generation. There is almost no transition region between the empty channel and the apparently undisturbed material including the MQW. This is in striking difference to the observations for GaAs-based materials.²⁴

5. Conclusions

A quantitative study is presented of the damage pattern caused by sudden degradation of GaN-based high-power diode lasers. Although the use of the term 'COD' in the introduction already implied the assumption that in GaN-based devices sudden degradation takes place within a positive feedback loop as in GaAs-based ones, we present independent experimental evidence for this.

- Defect growth during the process is feed by the optical mode; i.e. *laser energy*. In consequence, the damage pattern resembles the optical mode shape along its full extension along the z-axis.
- COD in GaN-based devices is a *hot process* that involves melting and even vaporization of MQW and waveguide materials. This indicates the presence of temperatures on the order of 2500-3000°C.

- Average defect propagation velocities along the z-axis of 110 m/s are observed.
- COD results in material loss including the formation of an *empty channel* that shows an utmost high uniformity along the z-axis. The presence of empty regions in the device is well consistent with material loss due to ejections of hot material out of the front facet of the device.⁴
- The laser structure in the immediate vicinity of the empty channel seems to be absolutely undisturbed. Down to a scale of a few nm (for sure $\ll 20$ nm), *there is no transition region* between empty channel and undisturbed original epitaxial layer sequence.

COD in GaAs- and GaN-based devices follow similar scenarios including the local attainment of the melting temperature by local absorption of laser light. The temperatures reached during COD in GaN-based devices are higher than observed for GaAs-based, owed to the different melting temperatures of the materials. The damage pattern differs substantially: We find a completely empty channel at the position of the optical mode that is surrounded by absolutely intact material, while earlier studies in GaAs-based devices, degraded under almost identical conditions, revealed molten, phase segregated, and both recrystallized and amorphous materials with well-pronounced melting fronts.²⁴ Propagation velocities of defect fronts in degrade GaN-based devices are faster, possibly again an effect caused by higher temperatures and substantially higher pressures.

Acknowledgements

One of the authors, JWT, wishes to thank Dr. Anna Mogilatenko for helpful discussions.

References

- [1] Tomm, J. W., Ziegler, M., Hempel, M., and Elsaesser, T., "Mechanisms and fast kinetics of the catastrophic optical damage (COD) in GaAs-based diode lasers," *Laser & Photonics Reviews*, 5(3), 422-441 (2011).
- [2] Harder, C., [Pump diode lasers] Elsevier, Amsterdam, 107-122 (2008).
- [3] Eliseev, P. G., "Optical strength of semiconductor laser materials," *Progress in Quantum Electronics*, 20(1), 1-82 (1996).
- [4] Hempel, M., Tomm, J. W., Stojetz, B., König, H., Strauss, U., and Elsaesser, T., "Kinetics of catastrophic optical damage in GaN-based diode lasers," *Semiconductor Science and Technology*, 30(7), 072001 1-6 (2015).

- [5] Ryu, H. Y., Ha, K. H., Lee, S. N., Choi, K. K., Jang, T., Son, J. K., Chae, J. H., Chae, S. H., Paek, H. S., Sung, Y. J., Sakong, T., Kim, H. G., Kim, K. S., Kim, Y. H., Nam, O. H., and Park, Y. J., "Single-mode blue-violet laser diodes with low beam divergence and high COD level," *Photonics Technology Letters, IEEE*, 18(9), 1001-1003 (2006).
- [6] Furitsch, M., [Untersuchung von Degradationsmechanismen an (Al/In)GaN-basierenden Laserdioden] Cuvillier-Verlag, Göttingen(2007).
- [7] Prystawko, P., Czernetzki, R., Gorczyca, L., Targowski, G., Wisniewski, P., Perlin, P., Zielinski, M., Suski, T., Leszczynski, M., Grzegory, I., and Porowski, S., "High-power laser structures grown on bulk GaN crystals," *Journal of Crystal Growth*, 272(1-4), 274-277 (2004).
- [8] Strauss, U., Somers, A., Heine, U., Wurm, T., Peter, M., Eichler, C., Gerhard, S., Bruederl, G., Tautz, S., Stojetz, B., Loeffler, A., and Koenig, H., "GaInN laser diodes from 440 to 530 nm: a performance study on single-mode and multi-mode R&D designs," *Proc. SPIE*, 10123, 101230A (2017).
- [9] Cooper, D. P., Gooch, C. H., and Sherwell, R. J., "Internal self-damage of gallium arsenide lasers " *IEEE Journal of Quantum Electronics*, QE 2(8), 329-330 (1966).
- [10] Zhang, Q., Xiong, Y., An, H., Boucke, K., and Treusch, G., "Unveiling laser diode "fossil" and the dynamic analysis for heliotropic growth of catastrophic optical damage in high power laser diodes," *Scientific Reports*, 6, 19011 1-12 (2016).
- [11] Hempel, M., Tomm, J. W., Hortelano, V., Michel, N., Jiménez, J., Krakowski, M., and Elsaesser, T., "Time-resolved reconstruction of defect creation sequences in diode lasers," *Laser & Photonics Reviews*, 6(6), L15-L19 (2012).
- [12] <http://www.lasershop.de/Laserquellen/Laserdioden/BLAUE-Laserdioden-86/OSRAM-Blau-Laserdiode-450nm-1-6W-PL-TB450.html>
- [13] Hempel, M., Tomm, J. W., Baeumler, M., Konstanzer, H., Mukherjee, J., and Elsaesser, T., "Near-field dynamics of broad area diode laser at very high pump levels," *AIP Advances*, 1(4), 042148 1-6 (2011).
- [14] M. Vanzi, Giansante, M., Zazzetti, L., Magistrali, F., Sala, D., Salmini, G., and Fantini, F., "Interpretation of Failure Analysis Results on ESD-Damaged InP Laser Diodes," 17th International Symposium for Testing and Failure Analysis & Microelectronics Symposium & Advanced Materials Symposium. 17 305-314 (1991).
- [15] Vanzi, M., Xiao, K., Marcello, G., and Mura, G., "Side-Mode Excitation in Single-Mode Laser Diodes," *IEEE Transactions on Device and Materials Reliability*, 16(2), 158-163 (2016).
- [16] Friede, S., Kuehn, S., Tomm, J. W., Hoffmann, V., Zeimer, U., Weyers, M., Kneissl, M., and Elsaesser, T., "Nano-optical analysis of GaN-based diode lasers," *Semiconductor Science and Technology*, 29(11), 112001 (2014).
- [17] Jacob, J. H., Petr, R., Jaspan, M. A., Swartz, S. D., Knapczyk, M. T., and Flusberg, A. M., "Fault protection of broad-area laser diodes," *Proc. SPIE*, 7198, 719815 1-10 (2009).

- [18] Hempel, M., La Mattina, F., Tomm, J. W., Zeimer, U., Broennimann, R., and Elsaesser, T., "Defect evolution during catastrophic optical damage of diode lasers," *Semiconductor Science and Technology*, 26(7), 075020 (2011).
- [19] Hempel, M., Tomm, J. W., Yue, F., Bettiati, M. A., and Elsaesser, T., "Short-wavelength infrared defect emission as a probe of degradation processes in 980 nm single-mode diode lasers," *Laser & Photonics Reviews*, 8(5), L59-L64 (2014).
- [20] Nakwaski, W., "Thermal model of the catastrophic degradation of high-power stripe-geometry GaAs/(AlGa)As double-heterostructure diode lasers," *Journal of Applied Physics*, 67(4), 1659-1668 (1990).
- [21] Henry, C. H., Petroff, P. M., Logan, R. A., and Merritt, F. R., "Catastrophic Damage of $\text{Al}_x\text{Ga}_{1-x}\text{As}$ Double-Heterostructure Laser Material," *Journal of Applied Physics*, 50(5), 3721-3732 (1979).
- [22] <http://www.ioffe.ru/SVA/NSM/Semicond/GaN/bandstr.html#Band%20wurtzite>
- [23] <http://www.ioffe.ru/SVA/NSM/Semicond/GaN/thermal.html>
- [24] Hempel, M., Tomm, J. W., La Mattina, F., Ratschinski, I., Schade, M., Shorubalko, I., Stiefel, M., Leipner, H. S., Kiessling, F. M., and Elsaesser, T., "Microscopic Origins of Catastrophic Optical Damage in Diode Lasers," *IEEE Journal of Selected Topics in Quantum Electronics*, 19(4), 1500508 1-8 (2013).

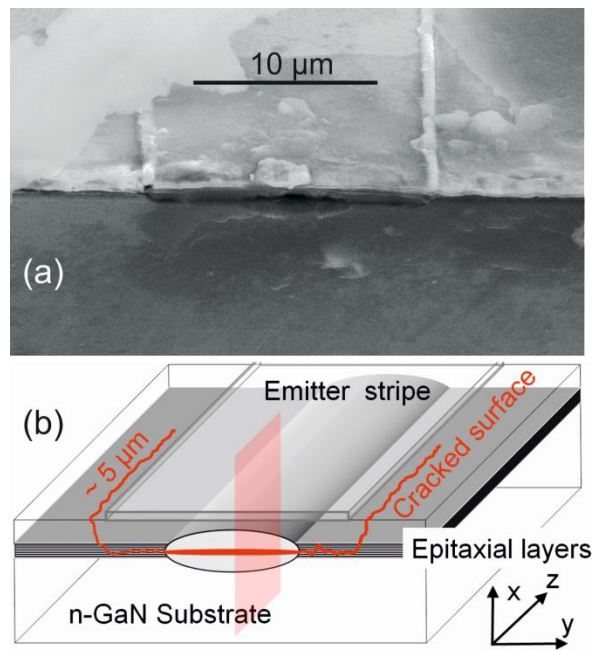


Figure 1 (a) COD pattern as observed by SEM at the front facet of a device. (b) Scheme illustrating the geometry of the device with the epitaxial layer on top, and the damage pattern. Cracks along the emitter stripes, including their extension along z-axis, are marked in red. The reddish plane illustrates the way how the FIB trenches (x-z-plane) that have been analyzed have been extracted. The coordinate system used is given, as well.

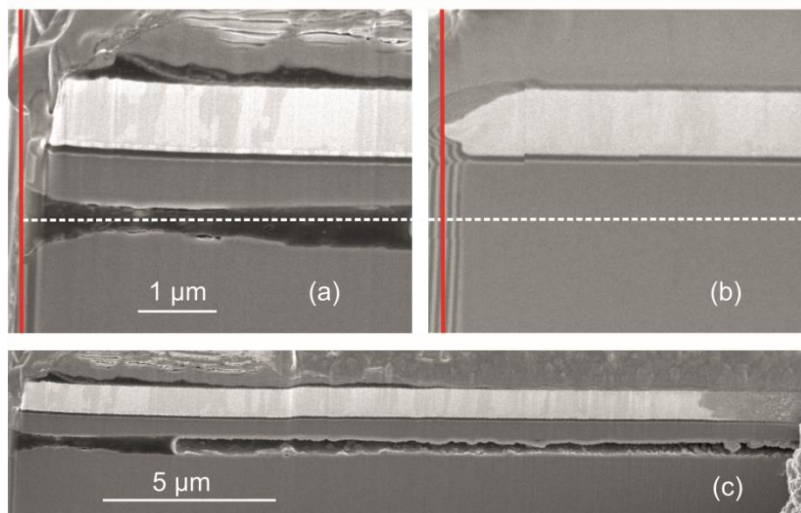


Figure 2 Comparison of SEM pictures from FIB lamellas (x-z-plane) at the front facet in an aged (a) and a pristine reference device (b). The front facet plane is marked by a red line, whereas the location of the QW-plane is indicated by a white dotted line. The bright $\sim 1 \mu\text{m}$ thick layer on top of the figures represents the p-metallization on top.

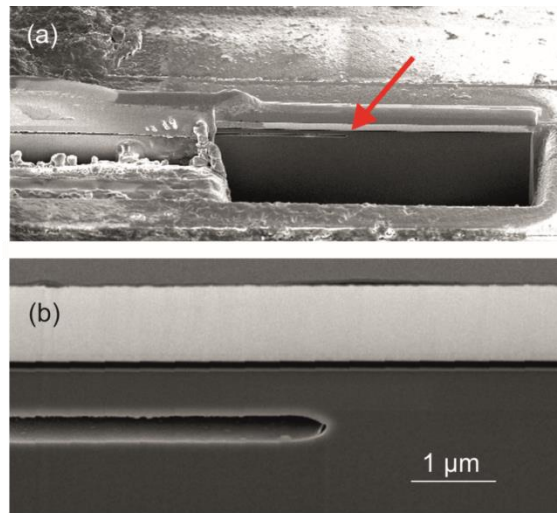


Figure 3 (a) SEM view to FIB trenches numbers 2 (left) and 3 (right), the latter fresh opened. The red arrow points to the end of the channel that has been created by the COD process. Note that the end of this channel is at $z=80\ \mu\text{m}$. (b) SEM view to the lamella extracted at FIB trench number 3 showing the end of the channel.

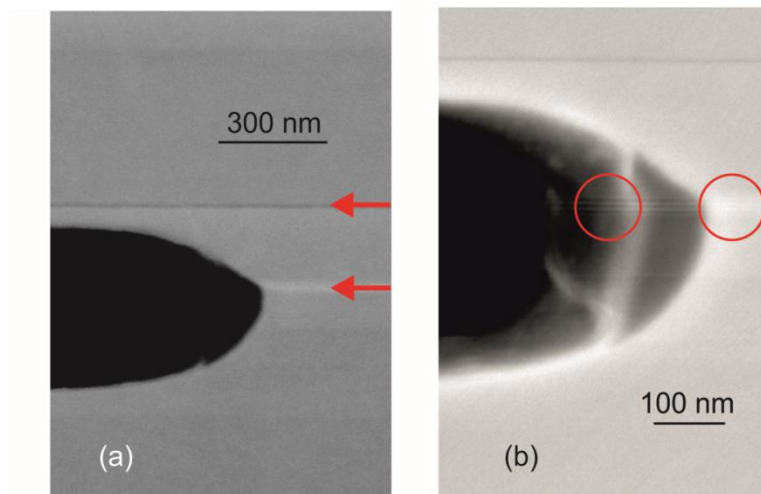


Figure 4 (a) STEM image of FIB trench number 3 at the end of the channel that has been created by the COD process. Red arrows mark the electron blocking layer (dark) and the MQW (bright), the latter still not resolved. (b) STEM image of FIB trench number 3 at the end of the channel. Here the MQW layers are clearly resolved. Both subfigures show the end of the channel exactly at the position of the MQW with a more pronounced widening towards the n- than towards the p-side.